SUPPORTING INFOMATION

***Thermus thermophilus* (*Tth*) σ^A**

Tth σ^A was prepared from *Escherichia coli* BL21(DE3) (Invitrogen, Inc.) transformed with plasmid pET28a-*Tth*σ^A, as in (1). *Tth* (Δ'513'-'519')σ^A, a derivative of Tth σ lacking residues 323-329 (which coorrespond to residues 513-519 of *Eco* σ^{70}), was prepared in the same manner from *Escherichia coli* BL21(DE3) transformed with plasmid pET28a-*Tth*σ^A(Δ'513'-'519') (prepared from plasmid pET28a-*Tth*σ^A by use of site-directed mutagenesis).

***Mycobacterium tuberculosis* (*Mtb*) RNAP σ^H**

Mtb σ^H was prepared from *E. coli* BL21(DE3) (Novoprotein, Inc.) transformed with plasmid pTolo-EX5-*Mtb*σ^H (2), as in (2).

***Tth* RNAP core enzyme**

Tth RNAP core enzyme was prepared from *Tth* strain HB8 (DSM579; Deutsche Sammlung von Mikroorganismen und Zellkulturen GmbH) as in (1).

***Mtb* RNAP core enzyme**

Mtb RNAP core enzyme was prepared from *E. coli* BL21(DE3) (Novoprotein, Inc.) transformed with plasmids pETDuet-*Mtb*-rpoA-rpoZ (2) and pACYCDuet-*Mtb*-rpoB-rpoC (2), as in (2).

***Tth* RNAP σ^A holoenzyme**

Tth RNAP holoenzyme was prepared as in (1). Briefly, *Tth* RNAP core enzyme (13 μM) and *Tth* σ^A or (Δ'513'-'519')σ^A (52 μM) were incubated in 2 ml 20 mM Tris-HCl, pH 7.7, 150 mM NaCl, and 2% glycerol for 1 h at 4 °C. The mixture was applied to a HiLoad 16/60 Superdex S200 column (GE Healthcare, Inc.) equilibrated in a running buffer of 20 mM Tris-HCl, pH 7.7, 100 mM NaCl, and 1% glycerol, and the *Tth* RNAP holoenzyme was eluted with the same buffer. Fractions containing *Tth* RNAP holoenzyme were pooled, concentrated to ~7.5 mg/ml using 30 kDa MWCO Amicon Ultra-15 centrifugal ultrafilters (Millipore, Inc.), and stored in the same buffer at -80 °C.

***Mtb* RNAP σ^L holoenzyme**

Mtb RNAP σ^L holoenzyme was prepared from *E. coli* strain BL21(DE3)STAR (Invitrogen, Inc.) transformed with plasmids pCOLADuet-*rpoB-rpoC (3-4)*, pACYC-*rpoA-sigL* [encodes *Mtb* RNAP α subunit and octahistidine-tagged *Mtb* σ^L; constructed from plamid pACYCDuet-*rpoA* (4) by deletion of the descahistidine-tag coding seqence preceding *rpoA* by use of site-directed mutagenesis (QuikChange II Site-Directed Mutagesesis Kit; Agilent, Inc.) and replacment of the BglII-XhoI DNA segment by the BglII-XhoI DNA segment of a DNA fragment, comprising 5'-ATGGCAGATCTAATGCATCATCATCATCATCATCATCAT-3' followed by codons 2-177 of *Mtb* σ^L followed by 5'- TGACTCGAG-3', generated by PCR using plasmid pSR32 (5) as template], and pCDF-*rpoZ* (4). Single colonies of the resulting transformants were used to inoculate 50 ml LB broth containing 100 μg/ml ampicillin, 35 μg/ml chloramphenicol, and 100 μg/ml streptomycin; cultures were incubated at 37°C with shaking until OD_{600} = 0.7; cultures were induced by addition of IPTG to 1 mM , and cultures were further incubated at 16 h 18°C with shaking. Cells were harvested by centrifugation (4,000xg; 10 min at 4°C), re-suspended in 50 ml buffer A (20 mM Tris-HCl, pH 8.0, 200 mM NaCl, 2 mM $ZnCl_2$, 1 mM EDTA, 5 mM 2-mercaptoethanol, and 5% glycerol) containing 1 tablet cOmplete Protease Inhibitor Cocktail (Roche, Inc.) at 4°C on ice; and lysed by sonication [4 min on ice; 4 s pulses at 40 W with 2 s intervals between pulses using Branson Ultrasonics Sonifier S-450A (Branson Ultrasonics, Inc.)]. The lysate was cleared by centrifugation (26,000 x g; 30 min at 4°C), and the cleared lysate (40 ml) was mixed with 2.8 ml 0.7% polyethyleneimine (Polymin-P; Sigma-Aldrich, Inc.), incubated 1 h with rotary shaking, and centrifuged (26,000xg; 10 min 4ºC). The polyethylene precipitate was washed 3 times by re-suspension in 40 ml buffer B (20 mM Tris-HCl, pH 8.0, 0.1 mM EDTA, 5 mM 2-mercaptoethanol, and 5% glycerol) containing 500 mM NaCl at 4°C, followed by centrifugation (26,000xg; 10 min at 4ºC), and was extracted with 20 ml buffer B containing 1 M NaCl at 4°C. The extract was cleared by centrifugation (26,000xg; 10 min at 4ºC), and the cleared extract was mixed with 30 ml ice-cold saturated ammonium sulfate, incubated 1 h with rotary shaking, and centrifuged (26,000xg; 30 min at 4ºC). The ammonium sulfate precipitate was dissolved in 30 ml buffer B containing 200 mM NaCl at 4°C, dialysed 16 h at 4°C against 2 L buffer B containing 200 mM NaCl, and an aliquot (30 ml) was applied to a 10 ml column of Ni-NTA agarose column (Qiagen, Inc.; pre-equilibrated in buffer B containing 200 mM NaCl; 4°C). The column was washed with 150 ml buffer B containing 200 mM NaCl and 15 mM imidazole, and was eluted with 20 ml buffer B containing 200 mM NaCl and 200 mM

imidazole. The eluate was applied to two tandem 5 ml HiTrap Q HP columns (GE Healthcare, Inc.; pre-equilibrated with buffer B containing 200 mM NaCl; 4°C; flow rate = 0.2 ml/min), the column was washed with 100 ml buffer B containing 200 mM NaCl, and the column was eluted with 200 ml of a linear gradient of 200-600 mM NaCl in buffer B at 4°C, and pooled fractions containing Mtb RNAP σ^L holoenzyme were concentrated to 5 ml using 30 kDa MWCO Amicon Ultra-15 centrifugal ultrafilters (Millipore, Inc.). The sample was further purified by gel filtration on a HiLoad 16/60 Superdex 200 prep grade column (GE Healthcare, Inc) in 20 mM Tris-HCl, pH 8.0, 75 mM NaCl, 5 mM $MgCl_2$, and 5 mM dithiothreitol, concentrated to 20 μM in the same buffer using 30 kDa MWCO Amicon Ultra-15 centrifugal ultrafilters, flash-frozen in liquid N2, and stored at -80°C. Yields were ~5 mg/L, and purities were >95%.

Nucleic-acid scaffolds

Oligodeoxyribonucleotides (IDT for *Tth* (Δ'513'-'519')σ^A-RPo, *Tth* σ^A-RPitcs, *Tth* σ^A-RPitcs-PPP, and *Mtb* σ^L-RPitc; Sangon Biotech for *Mtb* σ^H-RPitcs) and oligoribonucleotides (IDT for structures of *Tth* σ^A-RPitc, *Tth* σ^A-RPitc-PPP, and *Mtb* σ^L-RPitc; GenScript Biotech for *Mtb* σ^H-RPitc) were dissolved in ultrapure water (GIBCO) to 3 mM and stored at -80°C.

Nucleic-acid scaffolds (sequences in Fig. S1) for structures in Fig. 1-3 and S2 were prepared as follows. Nontemplate-strand DNA (0.5 mM final), template-strand DNA (0.55 mM final), and RNA [1 mM final; omitted for *Tth* σ^A-RPitc2-PPP and *Tth* (Δ'513'-'519')σ^A] were combined in 25 μl 5 mM Tris-HCl, pH 7.7, 200 mM NaCl, and 10 mM $MgCl_2$; were heated 5 min at 95°C; were cooled to 25°C in 2°C steps with 1 min/step using a thermal cycler (Applied Biosystems); and were stored at -80 °C.

Nucleic-acid scaffolds (sequences in Fig. S1) for structures in Fig. 4 were prepared as follows. Nontemplate-strand DNA (1 mM final), template-strand DNA (1 mM final), and RNA (1 mM final) were combined in 50 μl 5 mM Tris-HCl, pH 7.5; were heated 8 min at 95°C; cool to 22°C over 2 h, and were stored at -80°C.

Assembly of transcription initiation complexes

For structures in Figs. 1-2 and S2, complexes for crystallization were prepared by mixing 20 μl 18 μM *Tth* σ^A holoenzyme (in 20 mM Tris-HCl, pH 7.7, 100 mM NaCl, and 1% glycerol),

1 µl 0.5 mM nucleic-acid scaffold (in 5 mM Tris-HCl, pH 7.7, 200 mM NaCl, and 10 mM $MgCl_2$), and 1 µl 25 nM 5'-triphosphate-GpA (in water; *Tth* σ^A-RPitc2-PPP only), and incubating 1 h at 25°C.

For structures in Fig. 3, complexes for crystallization were prepared by mixing 500 µl 20 µM *Mtb* RNAP core enzyme (in 20 mM Tris-HCl, pH 7.7, 100 mM NaCl, and 1% glycerol), 120 µl 330 µM *Mtb* σ^H, and 30 µl 0.5 mM nucleic-acid scaffold (in 5 mM Tris-HCl, pH 7.7, 200 mM NaCl, and 10 mM $MgCl_2$), and incubating 12 h at 4 °C. The sample was loaded onto a Hiload 16/60 Superdex S200 column (GE Healthcare, Inc.) equilibrated in 10 mM Tris-HCl pH 8.0, 0.1 M NaCl, 1% (v/v) glycerol, 1 mM dithiothreitol at 4°C and eluted with 120 ml of the same buffer at 4°C. Pooled fractions containing *Mtb* σ^H-RPitc were concentrated to 7.5 mg/ml using 100 kDa MWCO Amicon Ultra-15 centrifugal ultrafilters (Millipore, Inc.) at 4°C.

For structures in Fig. 4, complexes for crystallization were prepared by mixing 20 µl 20 µM *Mtb* RNAP σ^L holoenzyme (in 20 mM Tris-HCl, pH 8.0, 75 mM NaCl, 5 mM $MgCl_2$, and 5 mM dithiothreitol) with 2 µl 1 mM nucleic-acid scaffold (in 5 mM Tris-HCl, pH 7.5), and incubating 20 min at 22°C.

Crystallization, data collection, and structure determination: *Tth* σ^A-RPitc and σ^A-RPitc-PPP

For structures in Figs. 1-2 and S2, crystallization was performed as in (1), but using the complexes of the preceding section. Briefly, crystallization drops containing 1 µl (Δ'513'-'519')σ^A-RPo or σ^A-RPitc (20 µM in 10 mM Tris-HCl, pH8.0, 100 mM NaCl, 0.5% glycerol, 1mM DTT), and 1 µl reservoir solution A [0.1 M Tris-HCl, pH8.0, 200 mM KCl, 50 mM $MgCl_2$, and 10% (m/v) PEG 4000] were equilibrated to 400 µl reservoir solution A in sealed hanging-drop plates. Crystals were grown 3 days at 22°C. Micro-seeding was performed as needed using the same reservoir solution. Crystals were transferred to reservoir solution A containing 18% (v/v) (2R, 3R)-(-)-2,3-butanediol (Sigma Aldrich) and flash-cooled in liquid nitrogen.

Diffraction data were collected at synchrotron beamlines CHESS-F1 and BNL-X25 and were processed using HKL2000 (6). Structures were solved by molecular replacement using the

crystal structure of *Tth* RPo (PDB 4G7H; 1) as search model. Iterative cycles of reciprocal refinement using Phenix (7) and real-space model building using Coot (8) were performed. The final atomic models and structure factors were deposited in the Protein Data Bank (PDB) with accession codes 6LTS, 6KQD, 6KQE, 6KQF, 6KQG, and 6KQH for *Tth* (Δ'513'-'519')σ^A-RPo, σ^A-RPitc3, σ^A-RPitc4, σ^A-RPitc5, σ^A-RPitc6, and σ^A-RPitc7, and with accession codes 6L74, 6KQL, 6KQM, and 6KQN for *Tth* σ^A-RPitc2-PPP, σ^A-RPitc4-PPP, σ^A-RPitc5-PPP, and σ^A-RPitc6-PPP, respectively (Tables S1-S2).

Crystallization, data collection, and structure determination: *Mtb* σ^H-RPitc

For structures in Fig. 3, crystallization was performed by mixing 1 µl *Mtb* σ^H-RPitc (20 µM in 10 mM Tris-HCl, pH8.0, 100 mM NaCl, 1% (v/v) glycerol, 1mM DTT) with 1 µl reservoir solution B [50 mM sodium cacodylate, pH 6.5, 80 mM magnesium cetate, and 15% (m/v) PEG 400]. Crystals were grown 1 week at 22°C in sealed hanging-drop plates, were cryo-protected in reservoir solution B containing 30% PEG 400, and were flash-cooled in liquid nitrogen.

Diffraction data were collected at Shanghai Synchrotron Radiation Facility (SSRF) beamlines 17U or 19U, and were processed using HKL2000 *(6)*. Structures were solved by molecular replacement using the crystal structure of *Mtb* σ^H-RPo (PDB 5ZX2; 2) as search model. Iterative cycles of reciprocal refinement using Phenix (7) and real-space model building using Coot (8) were performed. The final atomic models and structure factors were deposited in the PDB with accession codes 6KON, 6KOO, 6KOP, and 6KOQ for *Mtb* σ^H-RPitc5, σ^H-RPitc7, σ^H-RPitc9, and σ^H-RPitc10, respectively (Table S3).

Crystallization, data collection, and structure determination: *Mtb* σ^L-RPitc

For structures in Fig. 4, crystallization of *Mtb* σ^L-RPitc was performed by mixing 1 µl *Mtb* σ^L-RPitc (20 µM in 20 mM Tris-HCl, pH 8.0, 75 mM NaCl, 5 mM $MgCl_2$, and 5 mM dithiothreitol) with 1 µl reservoir solution C [100 mM sodium citrate, pH 5.6, 200 mM sodium acetate, and (m/v) 10% PEG 4000]. Crystals were grown at 1 week at 22°C in sealed hanging-drop plates, were cryo-protected in reservoir solution containing 20% (v/v) (2R, 3R)-(-)-2,3-butanediol, and were flash-cooled in liquid nitrogen.

Diffraction data were collected at Argonne Photon Source (APS) beamline 19-BM. Structures

were solved by molecular replacement usng the crystal structure of *Mtb* σ^L-RP_O (PDB 6DVC; *9*) as search model. One molecule of RNAP was present per asymmetric unit. Cycles of nodel building and refinement were performed using Coot (8) and Phenix (7). The final models were generated by X/Y/Z-coordinate refinement using secondary-structure restraints, followed by B-factor refinement and individual-B-factor refinement. The final atomic models and structure factors were deposited in the PDB with accession codes 6TYE, 6TYF, and 6TYG for *Mtb* σ^L-RPitc5, σ^L-RPitc6, and σ^L-RPitc9, respectively (Table S4).

REFERENCES

1. Y. Zhang *et al.,* Structural basis of transcription initiation. *Science* **338**(6110):1076-1080 (2012).
2. L. Li, C. Fang, N. Zhuang, T. Wang, Y. Zhang, Structural basis for transcription initiation by bacterial ECF sigma factors. *Nat Commun* **10**, 1153 (2019).
3. W. Lin*, et al.,* Structural Basis of *Mycobacterium tuberculosis* transcription and transcription inhibition. *Molecular cell* **66**(2):169-179 e168 (2017).
4. R. Banerjee, P. Rudra, R.K. Prajapati, S. Sengupta, J. Mukhopadhyay, Optimization of recombinant *Mycobacterium tuberculosis* RNA polymerase expression and purification. *Tuberculosis (Edinb)* **94**(4):397-404 (2014).
5. J.F. Jacques, S. Rodrigue, R. Brzezinski, L. Gaudreau, A recombinant *Mycobacterium tuberculosis in vitro* transcription system. *FEMS Microbiol Lett* **255**(1):140-7 (2006).
6. Z. Otwinowski, W. Minor W, [20] Processing of X-ray diffraction data collected in oscillation mode. *Methods Enzymol* **276**:307-326 (1997).
7. P. D. Adams*, et al.,* PHENIX: a comprehensive Python-based system for macromolecular structure solution. *Acta Crystallogr D Biol Crystallogr* **66**(Pt 2):213-221 (2010).
8. P. Emsley, K. Cowtan, Coot: model-building tools for molecular graphics. *Acta Crystallogr D Biol Crystallogr* **60**(Pt 12 Pt 1):2126-2132 (2004).
9. W. Lin *et al.* Structural basis of ECF-sigma-factor-dependent transcription initiation. *Nat Commun* **10**(1):710 (2019).

SUPPLEMENTAL TABLES

Table S1. Structure-determination and refinement statistics: *Tth* (Δ'513'-'519')σ^A-RPitc

	Tth **(Δ'513'-'519')σ^A-RPo**
Data collection	
Space group	C2
Cell dimensions	
a, b, c (Å)	183.7,103.8, 295.4
α, β, γ (°)	90.0, 98.6, 90.0
Resolution (Å)	45.00-3.45
R_{sym} or R_{merge} (%)	16.5 (69.5)
I/σI	8.5 (1.8)
Completeness	0.999 (0.992)
Redundancy	3.8 (3.5)
Refinement	
Resolution (Å)	45.00-4.45
No. reflections	72583
Rwork/ Rfree	22.0/25.8
No. of atoms	28227
Protein	27525
Nucleic acids	697
B-factors (Å^2)	101.2
Protein	99.7
Nucleic acids	157.3
R.m.s deviations	
Bond lengths (Å)	0.004
Bond angles (°)	1.006
Ramachandran plot	
Favored (%)	97.5
Allowed (%)	2.5
Disallowed (%)	0
PDB code	6LTS

Numbers in parentheses are for highest resolution.

Table S2. Structure-determination and refinement statistics: *Tth* σ^A-RPitc

	Tt **σ^A-RPitc3**	***Tt*** **σ^A-RPitc4**	***Tt*** **σ^A-RPitc5**	***Tt*** **σ^A-RPitc6**	***Tt*** **σ^A-RPitc7**
Data collection					
Space group	$P2_1$	C2	C2	C2	C2
Cell dimensions					
a, b, c (Å)	185.5, 104.0, 297.4	184.6, 103.8, 296.0	183.6, 103.6, 296.2	184.2, 104.0, 296.8	183.0, 103.6, 294.9
α, β, γ (°)	90.0, 98.5, 90.0	90.0, 98.7, 90.0	90.0, 98.9, 90.0	90.0, 98.6, 90.0	90.0, 99.2, 90.0
Resolution (Å)	50.00-3.30	50.00-3.30	50.00-2.45	50.0-2.80	40.0-3.20
R_{sym} or R_{merge}	9.2 (51.0)	13.2 (95.5)	9.2 (82.6)	7.4 (71.0)	18.5 (86.3)
I/σI	9.9 (1.6)	9.5 (1.2)	14.3 (1.7)	16.3 (1.4)	6.5/1.4
Completeness	0.916 (0.936)	1.00 (0.997)	0.999(0.998)	0.998 (0.980)	0.937 (0.911)
Redundancy	2.8 (2.7)	3.4 (3.3)	4.3 (3.5)	3.4 (3.0)	3.5 (3.3)
Refinement					
Resolution (Å)	50.00-3.30	50.00-3.30	50.00-2.45	50.00-2.80	40.00-3.20
No. reflections	154582	83410	201239	136907	85533
Rwork/ Rfree	20.7/24.9	21.8/25.8	19.9 (23.0)	20.5 (24.8)	20.3 (24.7)
No. of atoms	57053	28598	28634	28596	28589
Protein	55239	27671	27687	27607	27580
Nucleic acids	1825	932	953	995	1015
B-factors ($Å^2$)	83.1	96.0	64.6	88.6	64.7
Protein	82.3	95.2	63.6	87.9	63.8
Nucleic acids	107.7	120.9	94.4	108.7	87.8
R.m.s deviations					
Bond lengths (Å)	0.003	0.008	0.015	0.005	0.008
Bond angles (°)	0.617	1.074	1.026	0.735	0.632
Ramachandran plot					
Favored (%)	98.5	97.5	97.6	98.6	98.8
Allowed (%)	1.5	2.5	2.4	1.4	1.2
Disallowed (%)	0	0	0	0	0
PDB code	6KQD	6KQE	6KQF	6KQG	6KQH

Numbers in parentheses are for highest resolution.

Table S3. Structure-determination and refinement statistics: *Tth* σ^A-RPitc-PPP

	Tt **σ^A-RPitc2-PPP**	***Tt*** **σ^A-RPitc4-PPP**	***Tt*** **σ^A-RPitc5-PPP**	***Tt*** **σ^A-RPitc6-PPP**
Data collection				
Space group	C2	C2	C2	*C2*
Cell dimensions				
a, b, c (Å)	183.1, 103.5, 295.1	183.8, 103.2, 295.6	184.7, 102.7, 295.7	184.6, 101.9, 296.1
α, β, γ (°)	90.0, 99.2, 90.0	90.0, 99.1, 90.0	90.0, 98.9, 90.0	90.0, 98.8, 90.0
Resolution (Å)	45.00-3.10	45.00-2.88	50.00-3.20	50.00-3.50
R_{sym} or R_{merge}	14.1 (74.4)	11.0 (48.9)	14.1 (98.2)	13.7 (71.5)
I/σI	9.6 (1.6)	11.3 (2.4)	11.3 (1.5)	9.7 (1.5)
Completeness	0.999 (0.99)	0.999 (0.991)	0.998 (0.976)	0.950 (0.789)
Redundancy	3.6 (3.3)	3.7 (3.5)	5.2 (4.3)	4.6 (3.6)
Refinement				
Resolution (Å)	45.00-3.10	45.00-2.90	50.00-3.20	50.00-3.50
No. reflections	96614	121225	86387	64854
Rwork/ Rfree	19.1/23.6	20.7/24.6	20.5/25.2	21.3/25.8
No. of atoms	28744	28609	28642	28612
Protein	27685	27678	27691	27611
Nucleic acids	877	937	957	1007
B-factors (Å^2)	89.1	82.2	50.9	128.3
Protein	88.2	81.4	50.7	127.9
Nucleic acids	122.5	106.4	58.6	138.8
R.m.s deviations				
Bond lengths (Å)	0.009	0.010	0.008	0.008
Bond angles (°)	0.583	1.040	1.065	0.998
Ramachandran plot				
Favored (%)	98.1	98.0	97.4	97.7
Allowed (%)	1.9	2.0	2.6	2.3
Disallowed (%)	0	0	0	0
PDB code	6L74	6KQL	6KQM	6KQN

Numbers in parentheses are for highest resolution.

Table S4. Structure-determination and refinement statistics: *Mtb* σ^H-RPitc

	***Mtb* σ^H-RPitc5**	***Mtb* σ^H-RPitc7**	***Mtb* σ^H-RPitc9**	***Mtb* σ^H-RPitc10**
Data collection				
Space group	P21	P21	P21	P21
Cell dimensions				
a, b, c (Å)	129.3, 161.2, 129.5	125.0, 162.3, 128.5	127.4, 162.6, 133.4	126.9, 161.1, 129.6
α, β, γ (°)	90.0, 117.8, 90.0	90.0, 117.0, 90.0	90.0, 117.9, 90.0	90.0, 117.4, 90.0
Resolution (Å)	50.00-3.00	50.00-2.80	50.00-3.30	50-3.35
Rsym or Rmerge	10.5(107.2)	11.1(102.0)	11.9(154.7)	14.4(97.9)
I/σI	12.0(1.11)	14.4(1.1)	13.4(1.1)	10.9(1.2)
Completeness	0.978(0.88)	0.975(0.831)	0.986(0.992)	0.977(0.850)
Redundancy	4.2(3.6)	5.5(4.7)	4.2(4.2)	5.4(4.2)
CC1/2 in highest shell	0.506	0.608	0.502	0.600
Refinement				
Resolution (Å)	50.00-3.00	50.00-2.80	50.00-3.30	50.00-3.35
No. reflections	91412	109363	70820	64242
Rwork/ Rfree	22.1/27.1	20.6/24.8	21.7/25.5	22.1/26.0
No. of atoms	24039	24837	24560	24473
Protein	23117	23779	23450	23370
Nucleic acids	897	1029	1093	1082
B-factors (Å2)	95.42	88.28	121.84	103.06
Protein	94.08	87.80	121.78	102.44
Nucleic acids	130.47	99.94	125.3.71	117.02
R.m.s deviations				
Bond lengths (Å)	0.003	0.006	0.002	0.004
Bond angles (°)	0.554	0.765	0.514	0.661
Ramachandran plot				
Favored (%)	94.6	96.64	97.0	97.0
Allowed (%)	5.4	3.6	3.0	3.0
Disallowed (%)	0	0	0	0
PDB code	6KON	6KOO	6KOP	6KOQ

Numbers in parentheses are for highest resolution.

Table S5. Structure-determination and refinement statistics: *Mtb* σ^L-RPitcs

	***Mtb* σ^L-RPitc5**	***Mtb* σ^L-RPitc6**	***Mtb* σ^L-RPitc9**
Data collection			
Space group	P212121	P212121	P212121
Cell dimensions			
a, b, c (Å)	129.5, 158.5, 214.6	126.4, 161.7, 213.9	128.6, 158.2, 215.2
α, β, γ (°)	90.0, 90.0, 90.0	90.0, 90.0, 90.0	90.0, 90.0, 90.0
Resolution (Å)	48.01-3.30	49.26-3.30	49.12-2.92
Rsym or Rmerge	25.3(102.4)	18.6(89.4)	11.4(28.8)
I/σI	9.1(2.4)	5.6(1.1)	7.4(6.7)
Completeness	0.99(1.0)	0.95(0.98)	0.99(0.99)
Redundancy	9.0(8.7)	8.3(8.5)	6.8(8.6)
CC1/2 in highest shell	0.879	0.622	0.976
Refinement			
Resolution (Å)	48.01-3.80	49.26-3.80	49.12-3.50
No. reflections	42598	42516	55264
Rwork/ Rfree	25.2/30.3	24.8/30.6	24.1/29.5
No. of atoms	24794	24825	24818
Protein	23865	23834	23745
Nucleic acids	929	991	1073
B-factors (Å2)	91.66	89.54	73.09
R.m.s deviations			
Bond lengths (Å)	0.003	0.006	0.014
Bond angles (°)	0.635	0.768	1.149
Ramachandran plot			
Favored (%)	93.83	95.16	93.99
Allowed (%)	5.16	4.39	5.06
Disallowed (%)	1.01	0.46	0.95
PDB code	6TYE	6TYF	6TYG

Numbers in parentheses are for highest resolution.

SUPPLEMENTAL FIGURES

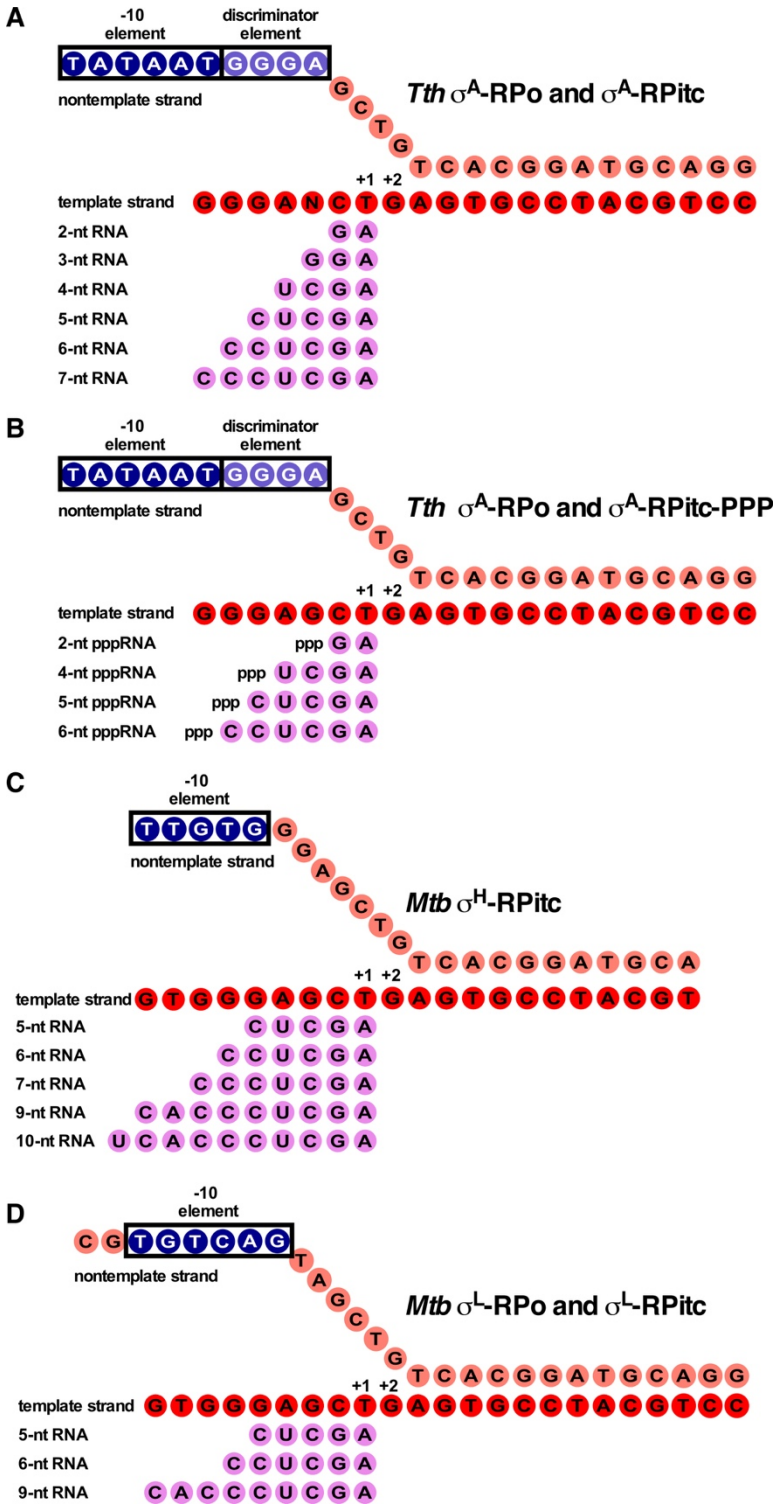

Figure S1. Nucleic-acid scaffolds used for structure determination in this study.

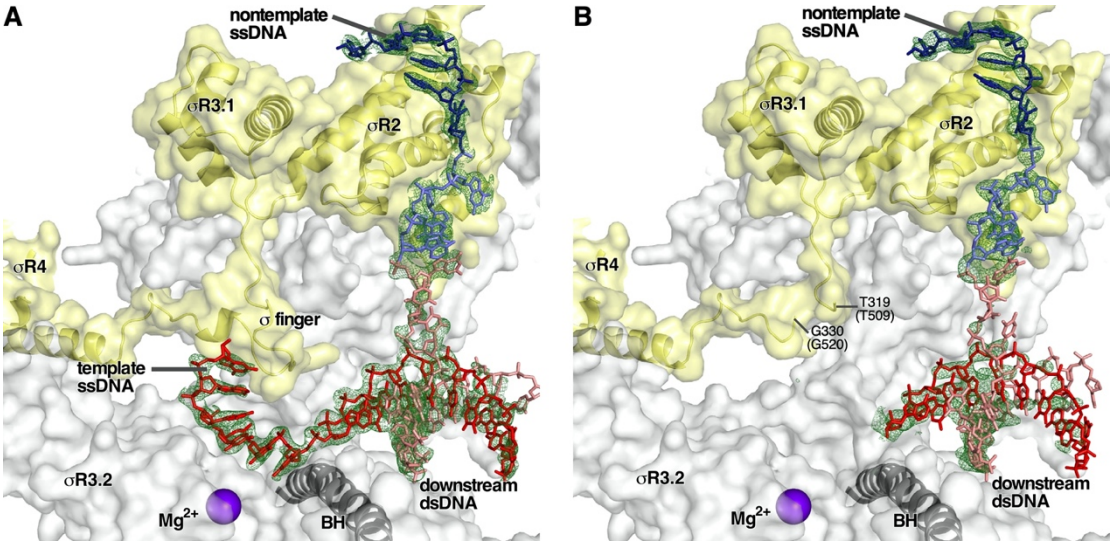

Figure S2. Deletion of σ finger results in segmental disorder of template-strand ssDNA, confirming that σ finger pre-organizes template-strand ssDNA to adopt ordered helical conformation and to engage RNAP active center.
(A) Structure of *Tth* σ^A-RPo (1; PDB 4G7O). Template-strand ssDNA adopts ordered helical conformation and engages RNAP active center (1). **(B)** Structure of *Tth* (Δ'513'-'519')σ^A-RPo (RPo containing σA derivative with deletion of residues that contact template-strand ssDNA; this work; Table S1). Template-strand ssDNA is segmentally disordered (no above-threshold electon density for temple-strand ssDNA nucleotides). White surfaces, solvent-accessible surfaces of RNAP β' subunit; yellow surfaces, solvent-accessible surfaces of σ; yellow ribbons, σ backbone; gray ribbon, RNAP bridge helix (BH); red sticks, template-strand DNA; blue, light blue and pink sticks, nontemplate strand DNA; purple sphere, RNAP active-center catalytic Mg^{2+} ion. Green mesh, simulated-annealing Fo-Fc electron density map contoured at 2.5 σ. σ residues are numbered as in *Tth* σ^A and, in parentheses, as in *Eco* σ^{70}.

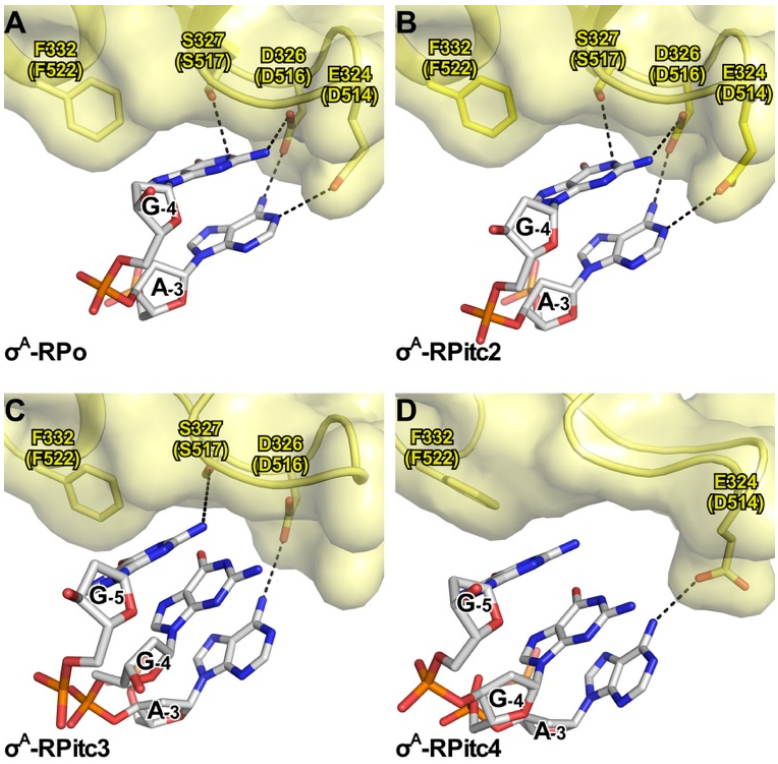

Figure S3. Pre-organization by σ finger of the template-strand ssDNA.
Interactions of σ finger with template-strand ssDNA in crystal structures of **(A)** *Tth* σ^A-RPo (PDB 4G7H) (1), **(B)** *Tth* σ^A-RPitc2 (PDB 4G7O) (1), **(C)** *Tth* σ^A-RPitc3 (this study), and **(D)** *Tth* σ^A-RPitc4 (this study). Yellow surfaces, solvent-accessible surfaces of σ; yellow ribbons, σ backbone; yellow and yellow-red stick representations, σ carbon and oxygen atoms; white, blue, red, and orange stick representations, DNA carbon, nitrogen, oxygen, and phosphorous atoms; black dashed lines, H-bonds. σ residues are numbered as in *Tth* σ^A and, in parentheses, as in *Eco* σ^{70}.

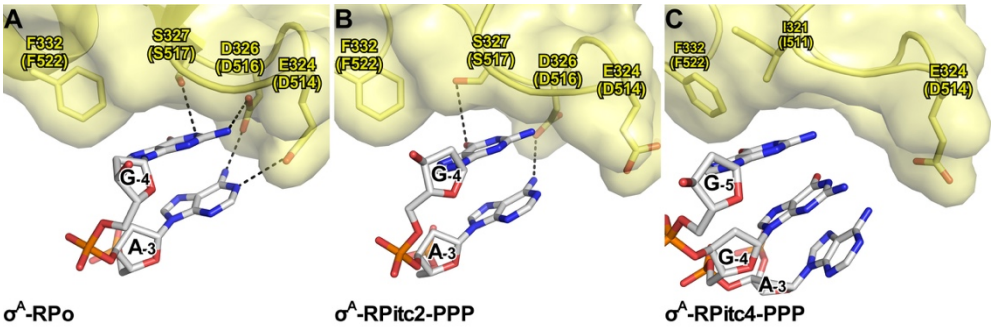

Figure S4. Pre-organization by σ finger of the template-strand ssDNA. The interaction of σ finger and template-strand ssDNA in crystal structure of **(A)** *Tth* σ^A-RPo (PDB 4G7H) (1), **(B)** *Tth* σ^A-RPitc2-PPP (this study), and **(C)** *Tth* σ^A-RPitc4-PPP (this study). Rendering and colors as in Fig. S3.

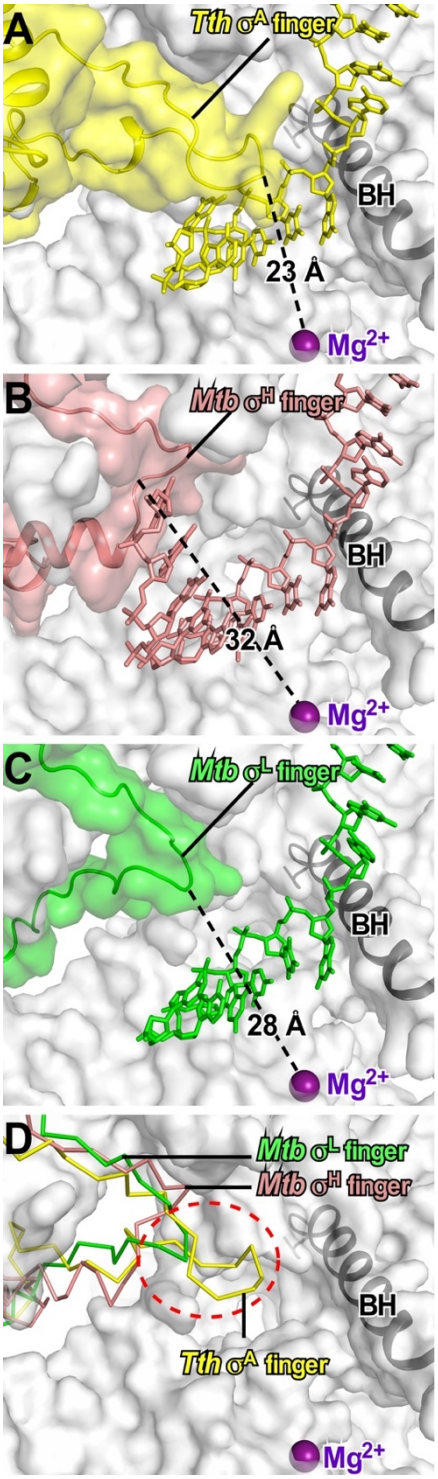

Figure S5. RNAP active-center region and σ finger for primary σ factor, σ^A (A), ECF σ factor σ^H (B), ECF σ factor σ^L (C), and superimposed σ^A, σ^H, and σ^L (D). RNAP active-center catalytic Mg^{2+} ion, purple sphere; RNAP active-center bridge helix (BH), gray ribbon; other RNAP residues, gray surface; σ finger, yellow, pink, and green ribbon plus surface for σ^A, σ^H, and σ^L, respectively (surfaces omitted in panel D); DNA template strand, yellow, pink, and green sticks for σ^A-, σ^H-, and σ^L-containing complexes, respectively (omitted in panel D). Distances between the tip of the σ finger and the RNAP active-center catalytic Mg^{2+} ion, are indicated in panels A-C. The red oval highlights the site where the σ fingers occupy in the RNAP active center.

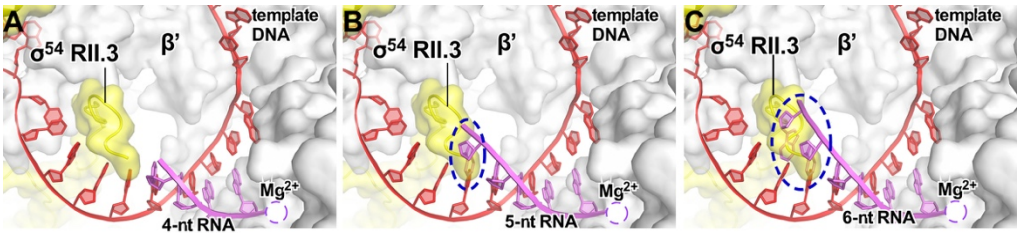

Figure S6. Predicted stepwise displacement of transcription-initiation-factor module in bacterial σ^{54}-dependent transcription initiation; collision of RNA 5' end with σ^{54} RII.3 upon extension of RNA from 4 nt to 5 nt. Rendering and colors analogous to rendering and colors in Figs 1-4. Dashed ovals, predicted steric clashes.

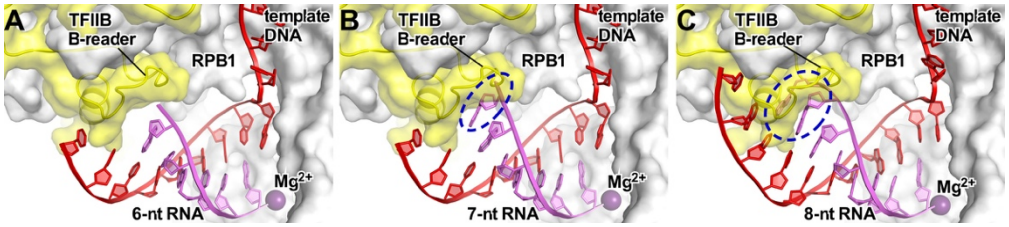

Figure S7. Predicted displacement of transcription-factor module in eukaryotic RNAP-II-dependent transcription initiation: predicted collision of RNA 5' end with TFIIB B-reader upon extension of RNA from 6 nt to 7 nt. Rendering and colors analogous to rendering and colors in Figs 1-4. Dashed ovals, predicted steric clashes.